Available online at www.sciencedirect.com

SciVerse ScienceDirect

Ceramics International 39 (2013) S633–S636

CERAMICS INTERNATIONAL

www.elsevier.com/locate/ceramint

Photoelectrochemical properties of $TiO_2/SrTiO_3$ combined nanotube arrays

Limin Guo, Xiaohui Wang*, Hui Zhang, Longtu Li

State Key Laboratory of New Ceramics and Fine Processing, Department of Materials Science and Engineering, Tsinghua University, Beijing 100084, China

Available online 17 October 2012

Abstract

The $TiO_2/SrTiO_3$ combined nanotube structure was obtained by the anodization and hydrothermal process. The as-prepared samples were characterized by X-ray diffraction, scanning electron microscopy, UV–vis absorption spectroscopy, etc. The behavior of photoelectrochemical activity in the combined films and pure TiO_2 nanotube arrays had been investigated through photo-to-current conversion efficiency measurement. Compared with bare TiO_2 electrodes, $SrTiO_3$ modified TiO_2 electrodes presented high charge transfer speed, high surface dominant photoelectrochemical response and photo-to-current conversion efficiency. The overall energy conversion efficiency was increased from 4.1% to 5.6% under the illumination of white light of 100 mW/cm^2 by using N719 dye. It demonstrates that the formation of a composite structure on surface of TiO_2 nanotubes plays an important role in the kinetic behaviors (like charge separation efficiency and electron transport rate) of the as-prepared DSSC cells. The mechanism for the enhancement of the photoelectrochemical activity is discussed.

Keywords: B. Nanocomposites; C. Electrical properties; D. TiO_2; E. Electrodes

1. Introduction

The interest in dye-sensitized solar cells (DSSCs) based on nanocrystalline porousTiO_2 has grown significantly due to the low cost, robust nature, environmental compatibility, and simplicity of the process [1]. In 1991, O'Regan and Grätzel first reported the dye sensitized nanocrystalline TiO_2 DSSC based on the mechanism of first regenerative photo-electrochemical processes with an efficiency of 7.1–7.9% [2]. Since then, extensive researches have continued to increase the power conversion efficiency of DSSC by incorporating other wide band metal oxide semiconductors such as ZnO, SnO_2, Nb_2O_5, etc and their composites as photoelectrode materials to achieve improved efficiency of DSSCs [3]. It is known that the recombination of photo-injected electrons in the conduction band of TiO_2 with the oxidized dye is one of the most important problems, especially in the films with small particles, many grain boundaries and relatively slow electron transport rate. The highly ordered TiO_2 nanotube (NT) films by a simple and green electrochemical anodization have shown many advantages in providing high surface area and efficient unidirectional charge transport routes, thus generating extensive technological interest [4–6]. The arrangement of the highly ordered TiO_2 NT array perpendicular to the surface permits facile charge transfer along the length of the NTs from the solution to the conductive substrate, thereby reducing the loss incurred by charge-hopping across the nanoparticle grain boundaries [7].

Recently, more and more researches focus on reducing recombination of photo-injected electrons at the interface by bilayers, composites, or passivation. This core–shell nano-structure could lower the charge recombination by building up an energy barrier at the semiconductor/electrolyte interface and, thus, retard the reaction between the photo-generated electrons and the redox species in electrolyte [8–10]. The shell layer should be more negative than that of the core in order to establish an energy barrier. Although many core–shell structure nanoparticles based DSSCs have been developed for enhancing the light conversion efficiency, few of them are related to the

*Corresponding author. Tel.: +86 1062784579; fax: +86 1062771160.
E-mail address: wxh@mail.tsinghua.edu.cn (X. Wang).

0272-8842/$ - see front matter © 2012 Elsevier Ltd and Techna Group S.r.l. All rights reserved.
http://dx.doi.org/10.1016/j.ceramint.2012.10.151

core–shell NT structure based DSSCs. In this paper, $TiO_2/SrTiO_3$ core–shell NT arrays were obtained by the anodization and hydrothermal reaction process. The effects of different reaction times on the essential structures and properties of the $TiO_2/SrTiO_3$ hybrid NTs were systematically investigated. The photo-electrochemical activity of the synthesized NTs was also tested.

2. Experiments

2.1. Preparation process

In a typical procedure, highly ordered TiO_2 NT array layers were prepared by anodization from the 99.7% Ti foil (10×15 mm^2) as described elsewhere in our early work [11]. The layers had a thickness of about 20 μm and a tubular diameter of around 200 nm. After annealing at 450 °C for 2 h, the samples were held at the center of teflon reaction vessels. The hydrothermal solution (0.0005 M strontium acetate and 0.001 M KOH) was prepared by CO_2-free deionized water and filled to 70% of the vessels. Then the vessels were placed into an oven heated at 180 °C for 3, 5 and 10 h. Finally, the samples were removed out, rinsed in deionized water and dried. Crystal structures of the specimens were determined by X-ray diffraction (XRD 2500, Rigaku, Tokyo, Japan). Microstructures of the NTs were observed by a field emission scanning electron microscope (FE-SEM, LEO-1530, LEO, Oberkochen, Germany). To obtain the information about band gap energy of the as-synthesized NTs, UV–visible absorption spectrum had been recorded using a fluorescence spectrophotometer (Varian Cary-Eclipse).

2.2. Photovoltaic characterization

The photovoltaic experiment of the NT arrays was performed as follows: after drying, photoanodes (TiO_2, $TiO_2/SrTiO_3$ NT arrays) were immersed in 5×10^{-3} M ethanol solution of the tetra-n-butylammonium dye (N719 dye, Dalian Seven Color Technology Co. Ltd., Dalian, China) for 24 h. Pt sputtered ITO glass was used as the counter electrode. The photovoltaic experiments were performed by the backside-illuminated method. The electrolyte comprised a mixture of 0.3 M LiI–0.03 M I_2–0.5 M TBP in an acetonitrile solution. The active area was 0.16 cm^2. Photovoltaic properties were measured under an AM1.5 solar condition and recorded by a source meter (Keithley-2400, Keithley Co. Ltd., Cleveland, OH).

3. Results and discussion

Fig. 1(a) shows the FE-SEM images of the as-prepared TiO_2 NT arrays anodic grown on Ti substrates. The layers consist of highly ordered NTs with an open porous structure at the top end. The diameters of the NTs range from 150 to 200 nm with smooth and straight walls (inset of Fig. 1(a)). Fig. 1(b)–(d) shows the FE-SEM images of

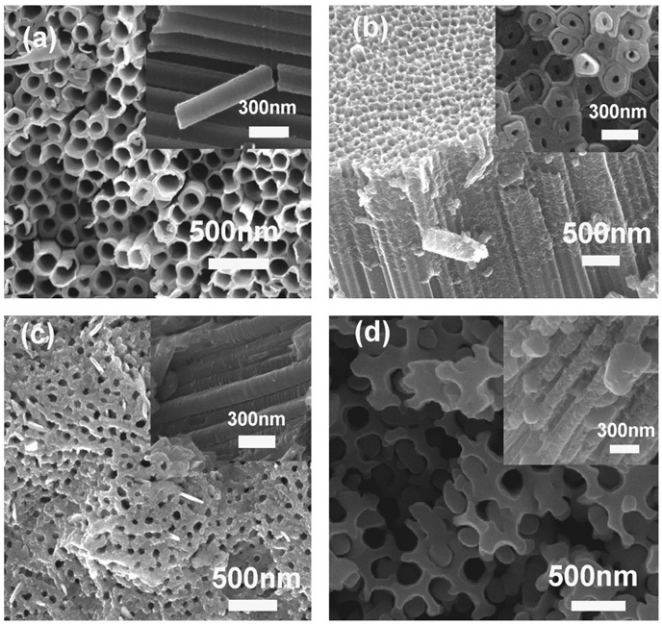

Fig. 1. SEM images of the as-prepared TiO_2 NT arrays (a) and samples after hydrothermal reaction at different times: 3 h (b), 5 h (c) and 10 h (d), and insets are the cross-section views of the films.

the NT arrays obtained after hydrothermal treatment of TiO_2 templates in 0.0005 M strontium acetate solutions with different reaction times. Minor differences are revealed for the samples obtained after hydrothermal reaction for 3 h (Fig. 1(b)). The tubal wall becomes a little thicker and rough. Obvious outer walls can be found in the space of the TiO_2 NTs (inset of Fig. 1(b) is the cross section view of the NTs at the bottom end). It could be explained by the crystal cell expansion during the formation of $SrTiO_3$ from TiO_2 and separation of these two phases [12].

Schematic illustration of the fabricating processes for the hybrid NTs is shown in Fig. 2(a). After hydrothermal treatment of the templates in solutions for 5 and 10 h, an ordered porous structure still existed in the layers. But evident distinctions are displayed. The obtained NT arrays collapse severely on the walls and the surface of the layer is overlaid by nano-scaled particles. Only a few pores can be found under the grainy layer (Fig. 1(c), (d)). This may not be favorable on their photo-electrochemical activity. The content ratio of $SrTiO_3/TiO_2$ in the films is 5.0%, 7.8% and 23% for reaction time of 3, 5 and 10 h respectively (calculated from the EDS spectra, Fig. 2(b)).

XRD patterns of the as-prepared samples before and after hydrothermal treatment are revealed in Fig. 3. Excluding some weak peaks according to hexagonal Ti substrate (marked with rotundities), all the positions of other peaks agree well with those of standard anatase TiO_2 (marked with pentacles) and cubic perovskite $SrTiO_3$ (marked with squares). The relative peak intensity of each phase has no obvious difference with the standard cards, which confirms that the NT layers have mainly polycrystalline structure with no preferred orientation.

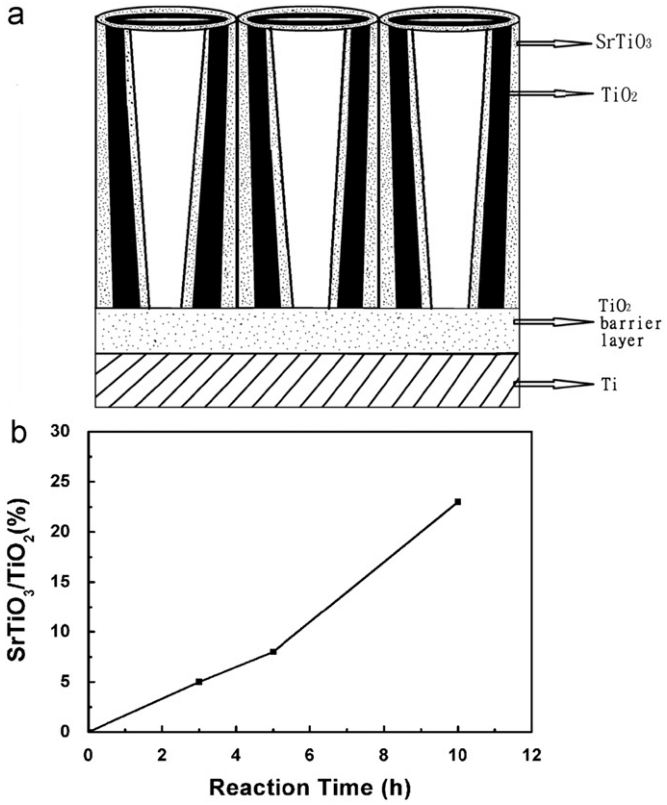

Fig. 2. Schematic illustration of the $SrTiO_3$ coated TiO_2 NTs (a) and content ratio of $SrTiO_3$ in the films obtained at different reaction times (b).

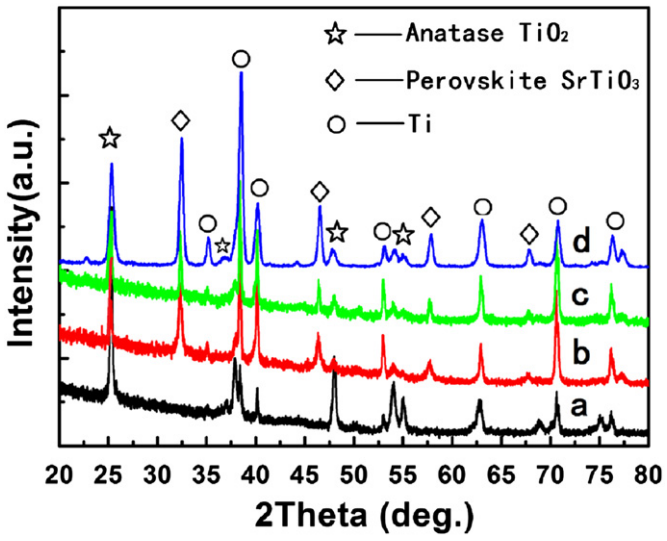

Fig. 3. XRD patterns of the as-prepared TiO_2 NT arrays annealed at 450 °C (a) and samples after hydrothermal reaction at different times: 3 h (b), 5 h(c) and 10 h (d).

But the intensity ratio for $SrTiO_3/TiO_2$ increases gradually with the hydrothermal reaction time (from 3 to 10 h). It indicates that the amount of $SrTiO_3$ shell has increment with the prolonging of reaction time. This agrees well with the results calculated from EDS spectra.

The UV–vis absorption spectra of the synthesized samples are shown in Fig. 4. All the samples show sharp absorption in UV region and high transparency in the visible region. But the absorption edge has some red-shift for the samples after hydrothermal reaction in strontium acetate solutions. Band edge of pure anatase TiO_2 phase is about 380 nm due to its intrinsic band gap of 3.23 eV. $SrTiO_3$ shell decorated TiO_2 NTs display broad absorption peaks with edges at about 390 nm and band gap was calculated as 3.21 eV.

Fig. 5 shows the comparison of I–V characteristics of the DSSCs based on TiO_2 NTs electrodes and $SrTiO_3$ coated TiO_2 NTs electrodes. The average photovoltaic parameters of samples measured under illumination AM 1.5 simulated sunlight (100 mW/cm^2) are summarized in Table 1. All the electrodes have the same thickness of 20 μm with N719 dye in liquid electrolyte medium. The hybrid electrodes showed a better performance than those of pure TiO_2 electrodes, which exhibit a higher short-circuit current density (J_{sc}) above 16 mA/cm^2 and an overall conversion efficiency (η) bigger than 5.2%. The TiO_2 NT electrodes show a J_{sc} of 10.2 mA/cm^2 and a η of 4.1%. The enhancement of J_{sc} for hybrid NT electrodes confirms the active role of $SrTiO_3$ in reducing the recombination by acting as an inherent energy barrier. Additionally, the electron injection rate may

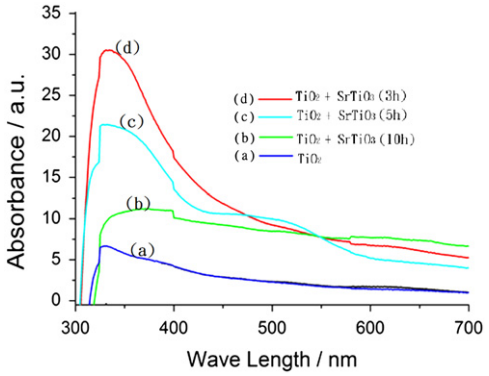

Fig. 4. UV–vis absorption spectra of TiO_2 NT arrays (a) and $SrTiO_3/TiO_2$ hybrid NT films after hydrothermal reaction at different times: 10 h (b), 5 h (c) and 3 h (d).

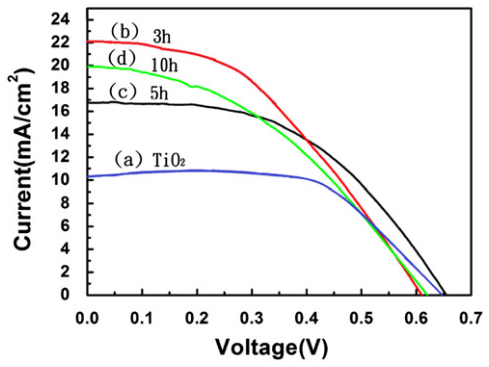

Fig. 5. Current–Voltage characteristics of bare TiO_2-based DSSC (a) and $SrTO_3/TiO_2$-based DSSCs after hydrothermal reaction at different times: 3 h (b), 5 h (c) and 10 h (d).

Table 1
Performance of DSSCs based on bare TiO_2 and $SrTiO_3$ coated TiO_2 systems.

Electrode–reaction time	J_{sc} (mA/cm^2)	V_{oc} (mV)	*FF*	η (%)
TiO_2	10.2	645	0.62	4.10
$SrTiO_3/TiO_2$–3 h	22	609	0.42	5.60
$SrTiO_3/TiO_2$–5 h	16.7	652	0.50	5.37
$SrTiO_3/TiO_2$–10 h	19.8	618	0.43	5.22

increase in the core–shell structure films by the perfect match between LUMO of dye molecules and the conduction band of electrodes achieved by a downward red-shift. The influence of $SrTiO_3$ coating on the fill factor (*FF*) of the DSSCs was also reviewed in Table 1. The *FF* value decreases in the $SrTiO_3$ doped NT electrodes, especially in the samples with a longer reaction time and higher $SrTiO_3$ contents. This is related to the bigger interface resistance between the electrode films and the Ti substrate induced by more micro-defects in the NT films obtained under a longer time. Further works for deeper processing of the $SrTiO_3/TiO_2$ NT arrays, investigating and enhancing their photovoltaic properties are underway.

4. Conclusion

The $TiO_2/SrTiO_3$ combined NT films were obtained by the anodization and hydrothermal process. The effects of reaction time on the $SrTiO_3$ content were studied and their solar cell performances were compared with those of undoped TiO_2 NTs. It was found that the $SrTiO_3$ shell was introduced into the interstitial sites of TiO_2 NTs and contributed to the red-shift of conduction band. The hybrid NT arrays showed an enhanced photovoltaic performance compared to those of undoped TiO_2. The enhanced photoelectric conversion efficiency could be attributed to the reducing recombination of photoelectron and bigger electron injection rate in the films due to the better matching to the LUMO of dye molecules and the barrier conduction band of the hybrid NTs.

Acknowledgements

The work was supported by Ministry of Sciences and Technology of China through National Basic Research Program of China (973 Program 2009CB623301), National Science Fund for Distinguished Young Scholars (Grant no. 50625204), Science Fund for Creative Research Groups (Grant no. 50921061), Outstanding Tutors for Doctoral Dissertations of S and T Project in Beijing (No.YB20081000302), and Tsinghua University Initiative Scientific Research Program.

References

[1] J.H. Yum, R. Humphry-Baker, S.M. Zakeeruddin, M.K. Nazeeruddin, M. Grätzel, Effect of heat and light on the performance of dye-sensitized solar cells based on organic sensitizers and nanostructured TiO_2, Nano Today 5 (2010) 91–98.
[2] B.O. Regan, M. Gratzel, A low-cost, high-efficiency solar cell based on dye-sensitized colloidal TiO_2 films, Nature 353 (1991) 737–750.
[3] R. Jose, V. Thavasi, S. Ramakrishna, Metal oxides for dye-sensitized solar cells, Journal of the American Ceramic Society 92 (2009) 289–301.
[4] Z. Miao, D.S. Xu, J.H. Ouyang, G.L. Guo, X.S. Zhao, Y.Q. Tang, Electrochemically induced sol − gel preparation of single-crystalline TiO_2 nanowires, Nano Letters 2 (2002) 717–720.
[5] M. Gratzel, Conversion of sunlight to electric power by nanocrystalline dye-sensitized solar cells, Journal of Photochemistry and Photobiology A: Chemistry 164 (2004) 3–14.
[6] R. Tenne, C.N.R. Rao, Inorganic nanotubes, Philosophical Transactions of the Royal Society A 362 (2004) 2099–2105.
[7] A. Subramanian, H.W. Wang, Effects of boron doping in TiO_2 nanotubes and the performance of dye-sensitized solar cells, Applied Surface Science 258 (2012) 6479–6484.
[8] J. Xie, T. Ji, X. Ou-Yang, Z. Xiao, H. Shi, Preparation of $SrTiO_3$ nanomaterial from layered titanate nanotubes or nanowires, Solid State Communications 147 (2008) 226–229.
[9] S. Yang, H. Kou, S. Song, H. Wang, W. Fu, The enhanced photoelectric conversion efficiency of N_3 sensitized $MgTiO_3$ modified nanoporous TiO_2 electrodes, Colloids and Surfaces A: Physicochemical and Engineering Aspects 340 (2009) 182–186.
[10] X. Zhang, K. Huo, L. Hu, Z. Wu, P.K. Chu, Synthesis and photocatalytic activity of highly ordered TiO_2 and $SrTiO_3/TiO_2$ nanotube arrays on Ti substrates, Journal of the American Ceramic Society 93 (2010) 2771–2778.
[11] Y. Yang, X. Wang, L. Li, Synthesis and photovoltaic application of high aspect-ratio TiO_2 nanotube arrays by anodization, Journal of the American Ceramic Society 91 (2008) 3086–3089.
[12] J. Zhang, J.H. Bang, C. Tang, P.V. Kamat, Tailored TiO_2–$SrTiO_3$ heterostructure nanotube arrays for improved photoelectrochemical performance, ACS Nano 4 (2010) 387–395.